Extended Abstracts of the 2016 International Conference on Solid State Devices and Materials, Tsukuba, 2016, pp213-214

D-5-03

Low-Temperature Gold-Induced Lateral Crystallization of Sn-Doped Ge on Insulator for Flexible Electronics

Takatsugu Sakai, Taizoh Sadoh, Ryo Matsumura, and Masanobu Miyao
Department of Electronics, Kyushu University, 744 Motooka, Fukuoka 819-0395, Japan
Phone: +81-92-802-3737 , E-mail : sadoh@ed.kyushu-u.ac.jp

Abstract

Low-temperature (≤250°C) formation of Sn-doped crystalline Ge on insulator is desired to realize next generation flexible electronics. To achieve this, gold-induced lateral crystallization of a-GeSn is investigated. For a-GeSn with initial Sn concentration of 5%, Sn-doped crystalline Ge is obtained at low temperatures (≤250℃). It is revealed that lateral crystallization is generated by diffusion of Au in GeSn. The Sn concentration (0.5−2.0%) in the grown layers can be controlled by the annealing temperature.

1. Introduction

A technique for low-temperature (≤250°C) formation of high-quality crystalline Ge films on insulator is expected to realize advanced high performance thin film transistors (TFT) on flexible plastic substrates (softening temperature: ~300ºC). To improve quality of Ge crystals, Sn-doping (<4%) is very effective, because it enables passivation of point defects in Ge [1]. This triggered the recent research of solid-phase crystallization of Sn-doped Ge (Sn concentration: 2%) on SiO_2 layers. However, the growth temperature (425°C) reported to date is higher than the softening temperatures of plastic substrates [2]. To decrease the growth temperature of Sn-doped Ge, in the present study, we investigate gold-induced lateral crystallization (GILC) of a-GeSn. As a result, crystalline GeSn with controlled Sn concentration (0.5−2.0%) is obtained at temperatures below 250°C.

2. Experiments and Results

Fig. 1 schematically shows the sample preparation procedure. Amorphous $Ge_{1-x}Sn_x$ layers (x: 0−0.2, thickness: 100 nm) were deposited on quartz substrates, and Au island patterns (thickness: 100 nm, diameter: 500 μm) were formed on the a-GeSn layers. The samples were annealed at 150−250ºC to induce lateral growth.

Figs. 2(a) and 2(b) show Nomarski optical micrographs of $Ge_{1-x}Sn_x$ (x: 0.05 and 0.1, respectively) samples after annealing (250ºC, 10 min). Here, Au pattern regions are located in the left side areas of the micrographs. For $Ge_{0.95}Sn_{0.05}$ sample, different contrast regions are observed around Au patterns, as indicated by the broken lines. On the other hand, for $Ge_{0.9}Sn_{0.1}$ sample, no change occurs after annealing. Raman spectra obtained at points #1−3 in Figs. 2(a) and 2(b) are shown in Fig. 2(c). Only in Raman spectra #1 ($Ge_{0.95}Sn_{0.05}$), a sharp peak due to Ge-Ge bonding in c-Ge is observed. These results indicate that GILC is generated for $Ge_{0.95}Sn_{0.05}$ sample, while it does not occur for $Ge_{0.9}Sn_{0.1}$ sample.

Lateral growth lengths at 150−250ºC for samples (Sn concentration: 0, 5, 10, 20%) are summarized as a function of the annealing time in Fig. 3. For low Sn concentrations (≤5%), lateral growth lengths steeply increase and seem to saturate in a short annealing time (10 min). The growth lengths increase with increasing temperature. To investigate distribution of Au in grown layers, Auger electron spectroscopy (AES) measurements were performed. Figs. 4(a), 4(b), and 4(c) show SEM image, lateral, and in-depth concentration profiles of Au, respectively, for $Ge_{0.95}Sn_{0.05}$ sample after annealing (250ºC, 60 min). Here, lateral and in-depth profiles were obtained along line A−B and point #1, respectively, shown in Fig. 4(a). The lateral profile [Fig. 4(b)] shows Au concentration on the surface of the sample. Fig. 4(b) indicates that Au atoms are diffused from Au pattern into laterally grown region. On the other hand, Fig. 4(c) indicates that Au atoms are localized near surface. These results indicate that lateral-growth of a-GeSn is generated by Au diffusion in the near surface regions of a-GeSn layers, followed by crystallization in vertical direction, in short time annealing (≤60min).

To examine the validity of the diffusion mechanism, Fig. 5(a) shows growth lengths after long annealing time (t). The apparently saturated growth lengths shown in Fig. 3 is found to increase for t >10 min. Fig. 5(b) shows increase in growth length (ΔL) as a function of the square root of the annealing time ($\sqrt{t-t_1}$), where the increase of the growth length from t_1 = 10 min is plotted. The good linear fitting in Fig. 5(b) indicates that slow lateral growth shown in t > 10 min is attributed to Au diffusion through crystallized Ge.

Substitutional Sn concentrations in grown layers for $Ge_{0.95}Sn_{0.05}$ samples, evaluated by the shift of the Raman peaks, are summarized as a function of the annealing temperature in Fig. 6(a). Substitutional Sn concentrations change from 0.5% to 2.0% with increasing temperature from 150°C to 250°C. These values show good agreement with the temperature dependent solubility, shown by the broken line. This indicates that the substitutional Sn concentration can be well controlled by the temperature, which is useful to passivate point defects in Ge [1]. Post annealing effects (250°C) on the substitutional Sn concentrations are summarized in Fig. 6(b). This guarantees the thermal stability of the substitutional Sn atoms over a long time annealing (>3000 min).

3. Conclusion

GILC of a-GeSn has been investigated. Sn-doped crystalline Ge is formed at low temperatures (≤250°C) by Au-diffusion in GeSn. The annealing temperature controlled substitutional Sn concentrations (0.5−2.0%) with high thermal stability (>3000 min) are observed. This technique will facilitate realization of flexible electronics.

References

[1] O. Nakatsuka, et al., JJAP **49**, 04DA10 (2010).

[2] W. Takeuchi, et al., APL **107**, 022103 (2015).

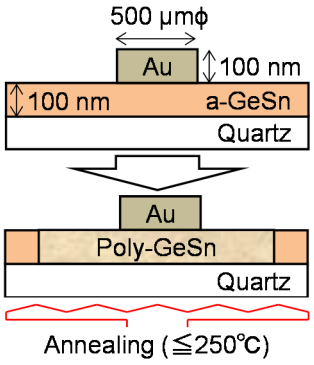

Fig.1. Schematics of sample preparation.

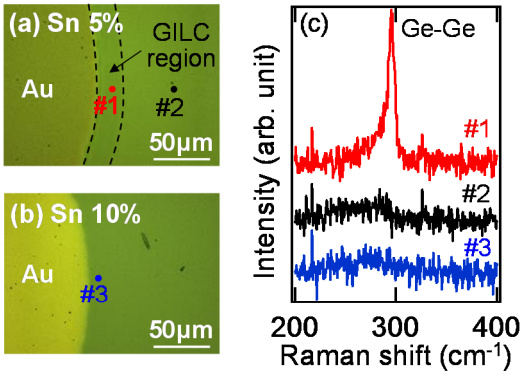

Fig.2. Nomarski optical micrographs [(a), (b)] and Raman spectra (c) for samples with initial Sn concentration of 5% and 10%. The annealing was performed at 250°C for 10 min.

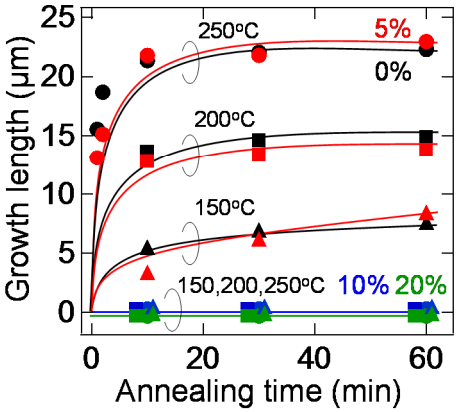

Fig.3. Lateral growth length for samples with Sn concentrations (0, 5, 10, 20%) as a function of annealing time.

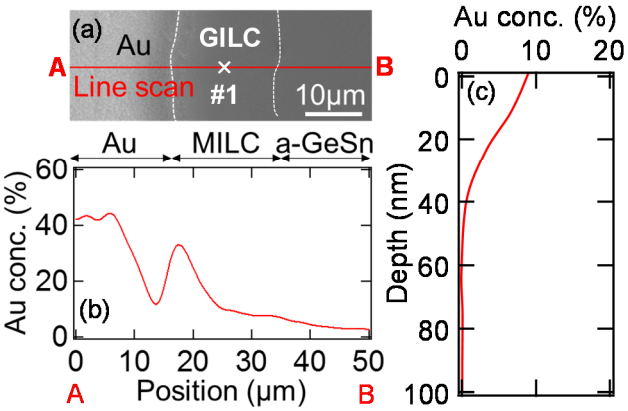

Fig.4. SEM image (a), lateral (b), and in-depth Au concentration profiles (c) of sample (initial Sn concentration: 5%) after annealing (250°C, 60 min). (b) and (c) were obtained by AES along line A−B and point #1, respectively, shown in (a).

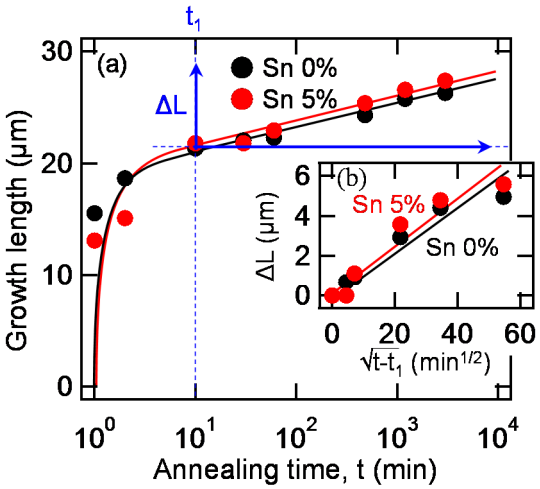

Fig.5. Lateral growth length at 250°C as a function of annealing time t (a) and increase in growth length ΔL after t_1 (10 min) as a function of square root of annealing time $\sqrt{t-t_1}$ (b).

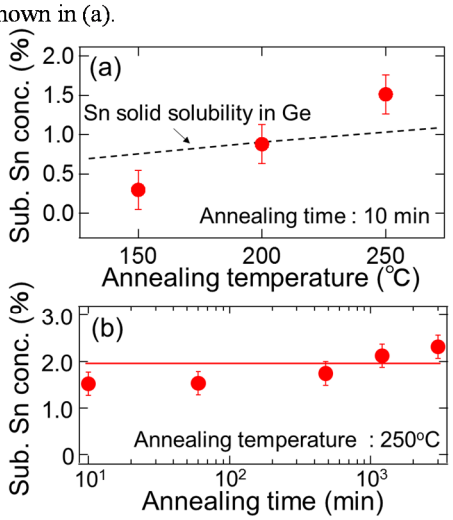

Fig.6. Substitutional Sn concentration for samples (initial Sn concentration: 5%) as a function of annealing temperature (a) and annealing time (b).